HHS Public Access

Author manuscript

Opt Lett. Author manuscript; available in PMC 2018 June 04.

Published in final edited form as:

Opt Lett. 2018 April 15; 43(8): 1914–1917.

Three-photon fluorescence microscopy with an axially elongated Bessel focus

Cristina Rodríguez[1], **Yajie Liang**[1], **Rongwen Lu**[1], and **Na Ji**[1,2,*]

[1]Janelia Research Campus, Howard Hughes Medical Institute, Ashburn, Virginia 20147, USA

[2]Department of Physics, Department of Molecular & Cellular Biology, University of California, Berkeley, California 94720, USA

Abstract

Volumetric imaging tools that are simple to adopt, flexible, and robust, are in high demand in the field of neuroscience, where the ability to image neurons and their networks with high spatiotemporal resolution is essential. Using an axially elongated focus approximating a Bessel beam, in combination with two-photon fluorescence microscopy, has proven successful at such an endeavor. Here we demonstrate three-photon fluorescence imaging with an axially extended Bessel focus. We use an axicon-based module which allowed for the generation of Bessel foci of varying numerical aperture and axial length, and apply this volumetric imaging tool to image mouse brain slices and for *in vivo* imaging of the mouse brain.

Two-photon fluorescence microscopy [1] has proven to be an invaluable tool for neuroscience, allowing for the study of neural structure and activity deep inside the living brain. More recently, three-photon fluorescence microscopy, in combination with long wavelength excitation, has been shown to push the depth limits of nonlinear imaging in scattering brain tissue [2, 3] and has allowed for transcutical imaging of the fly brain [4]. An attractive feature of these multiphoton imaging modalities relies in their optical sectioning capabilities. Since the excitation is localized to a small volume (on the order of a wavelength) around the focal point, intrinsic 3D resolution is achieved. Neurons and their networks, however, can extend over hundreds of micrometers in three dimensions. In order to image a volume using a standard multiphoton fluorescence microscope, a stack of images at different depths must be obtained. Consequently, the volumetric acquisition speed is highly compromised, making it difficult to capture dynamic events, such as calcium transients [5], with subsecond temporal resolution. The need for faster volumetric imaging tools has motivated the design and implementation of a number of technologies [6]. Among them is the generation of an axially extended focus approximating a Bessel beam, by illuminating the back aperture of the excitation objective with an annulus of light [7]. With this approach, a projected view of the 3D volume is obtained, with a volume rate equivalent to the frame rate, without compromising the lateral resolution. Several approaches have been demonstrated for generating a Bessel beam under two-photon excitation. The most common

*Corresponding author: jina@berkeley.edu.

OCIS codes: (170.3880) Medical and biological imaging; (180.2520) Fluorescence microscopy; (190.4180) Multiphoton processes.

approach involves the use of an axicon (conical lens) [8, 9, 10]. Other approaches employed a phase mask [11], or alternatively a spatial light modulator (SLM) [12], with the latter allowing for great flexibility in generating different types of Bessel foci with shaped axial intensity profiles.

In this paper, we demonstrate, for the first time to our knowledge, three-photon fluorescence imaging with an axially extended focus. We employ a flexible axicon-based Bessel module and demonstrate the generation of Bessel foci of different axial extents under three-photon excitation, and apply this volumetric imaging tool to image mouse brain slices and for *in vivo* imaging of the mouse brain.

A simplified diagram of our homebuilt three-photon microscope is shown in Fig. 1(a). The three-photon excitation source consists of a two-stage optical parametric amplifier (Opera-F, Coherent) pumped by a 40 W diode-pumped femtosecond laser (Monaco, Coherent), providing a broad tuning range (650-900 nm and 1200-2500 nm). For the experiments presented here, Opera-F was operated at 1300 and 1700 nm, for which the average output power was ~1.5 and ~0.9 W (1.5 and 0.9 μJ per pulse at 1 MHz repetition rate), respectively. For 1300 nm excitation, to reduce the group delay dispersion (GDD) at the sample plane, a homebuilt single-prism compressor was used [13]. The pulse duration at the focal plane of the objective was measured to be ~54 fs after compensation. For 1700 nm excitation, since the GDD is anomalous for many of the glasses used in our microscope, we cannot use our prism-based compressor to compensate for the resulting negative GDD at the sample plane. Instead, we used the high normal dispersion of ZnSe (from a bulk compressor available inside Opera-F) and silicon (from a 3-mm thick window placed at Brewster's angle[14]) to obtain a pulse duration at the sample of ~70 fs after compensation. A Pockel cell was used for controlling the power. A pair of galvanometers that were optically conjugate to each other and the back focal plane of a high-numerical aperture (NA) objective (Olympus XLPLN25XWMP2, NA 1.05, 25×) steered the excitation focus in the xy plane. The objective was mounted on a piezoelectric stage (PIFOC, Physik Instrumente) to translate the focus axially. The fluorescence signal is collected by the same objective and reflected from a dichroic beam splitter, spectrally filtered, and detected by a photomultiplier tube (Hamamatsu).We used D2O, instead of H2O, for the objective immersion media, because of its much lower absorption at the wavelengths of interest, particularly at 1700 nm [14]. Custom-written software was used for image acquisition.

To generate a Bessel focus, we placed an axicon-based module before the scanning unit, as shown in Fig. 1(a). The module consists of an axicon (apex angle of 178°) followed by a lens (L_1), which transforms the incident laser beam into an annulus of light. This annulus is imaged into the galvanometers (by the lens pair L_2 and L_3) and back focal plane of the objective, generating an axially elongated focus at the sample plane. An annular mask is placed at the back focal plane of lens L_1 to block unwanted light arising from imperfections of the axicon. By changing the focal length of lens L_1, the NA of the Bessel beam can be adjusted. Additionally, lens L_2 can be translated along its optical axis, allowing for the adjustment of the effective NA as well as the axial length of the Bessel focus [10]. Here, moving lens L_2 towards the mask (negative offset value) generates a longer Bessel focus;

whereas moving lens L_2 away from the mask (positive offset value) results in a shorter Bessel focus.

To illustrate the versatility of our Bessel module to generate Bessel foci of different NAs and consequently axial lengths, we imaged a 1-μm red fluorescent bead (Fluosphere; Invitrogen) using three different Bessel foci with an axial full width at half maximum (FWHM) ranging from 20 to 90 μm, as shown in Fig. 1(b).

Previous observations showed that, for two-photon fluorescence microscopy, lower-NA (e.g., 0.4 or 0.6) Bessel foci produced better-quality images of brains *in vivo* [12]. For high-NA Bessel foci (e.g., 0.9), more energy is distributed in the side rings, causing a stronger background and image blur. Due to its higher nonlinearity, three-photon excitation should more effectively suppress the fluorescence signal generated by the side rings of a high-NA Bessel focus than two-photon excitation. Indeed, as illustrated in Fig. 1(c), the lateral (xy) images of a 0.2-μm red fluorescent bead (Fluosphere; Invitrogen)which were obtained using two- and three-photon excitation, respectively, showed substantially reduced side-ring signal via three-photon excitation under 1300 nm excitation for a 0.96-NA Bessel focus, as shown in their radially averaged intensity profiles in Fig. 1(d). (A titanium-sapphire laser - Chameleon Ultra II, Coherent -operating at 920 nm was used as the two-photon excitation source.)

Having demonstrated the ability to generate Bessel foci under three-photon excitation, we applied this technique to image mouse brain slices (Thy1-GFP line M) using 1300 nm excitation. As demonstrated in Fig. 2, using a Bessel focus with axial FWHM of 36 μm and 0.6 NA, we were able to image neural structures extending ~50 μm in depth in a single frame. In Fig. 2(b), the Bessel image captured the basal dendrites surrounding the neuronal cell body; in Fig. 2(d), the Bessel image resolved fine dendrites and dendritic spines over a similar volume. In comparison, a Gaussian focus, generated by overfilling the back aperture of the 1.05 NA microscope objective with 1300 nm excitation, has an axial FWHM of ~1.8 μm under three-photon excitation. In order to capture all the structures in the same volume as that obtained with a Bessel focus, as shown in Figs. 2(b) and 2(d), we acquired ~50-μm thick image stacks made of 26 frames (Figs. 2(a) and 2(c), color-coded by depth), with 2-μm axial step size. Comparing the Gaussian and Bessel images indicates that finer structures visible in the Gaussian stacks were clearly resolved using the Bessel imaging modality (arrowheads in Figs. 2(c) and 2(d)). Therefore, for three-photon fluorescence microscopy, scanning a Bessel focus captures all features of interest in a volume in a single frame, without compromising the lateral resolution.

Imaging biological structures *in vivo* is one of the most valuable applications of optical microscopy, allowing for the study of biological systems in a relatively undisturbed and more physiological state. Figure 3 shows representative images taken during *in vivo* three-photon imaging of the mouse brain (Thy1-GFP line M and Gad2-IRES-Cre × Ai14 for 1300 and 1700 nm excitation, respectively).Under 1300 nm excitation, using a Bessel focus having an axial FWHM of 38 μm and 0.6 NA, we were able to probe neural structures extending over 60 μm *in vivo* in a single frame, as displayed in Figs. 3(b) and 3(d), while maintaining the lateral resolution to resolve synaptic structures such as dendritic spines

(white arrowheads) and axonal boutons (yellow arrowheads). Under 1700 nm excitation, using a Bessel focus with axial FWHM of 27 μm and 0.6 NA, we were able to capture neuronal cell bodies extending ~30 μm in depth in a single frame, as shown in Fig. 3(f). Similar to our observations in brain slices, all the neuronal structures observable in the image stacks obtained with a Gaussian focus were clearly identifiable using the Bessel imaging modality. Due to small tilts of the Bessel beam relative to the Gaussian beam, images obtained with the Bessel focus show a slightly different perspective than those obtained with the Gaussian focus.

It is important to note that glass cranial windows, used for providing optical access into the mouse brain, introduce aberrations. If not compensated for, such aberrations have a detrimental effect on the image quality. Here, we used the correction collar of the objective to compensate for the spherical aberration introduced by the glass window. Furthermore, to avoid the additional aberration modes that arise from a tilted cranial window (e.g., coma, astigmatism) [15], we carefully positioned the mouse using the third-harmonic signal from the glass window interfaces to check and correct for any tilt. For application in deeper depths, one needs to utilize adaptive optics to correct for the sample-induced aberrations [4, 16, 17].

We have demonstrated three-photon fluorescence imaging with an axially extended focus, under both 1300 and 1700 nm excitation for green and red fluorophores, respectively. An axicon-based Bessel module was incorporated into a homebuilt three-photon microscope, which allowed for the generation of Bessel foci of varying NA and axial extents. When compared to two-photon excitation, three-photon excitation was shown to more effectively suppress the signal associated with side rings of high-NA Bessel foci. Both in fixed slices and *in vivo*, three-photon excitation fluorescence microscopy using a Bessel focus allowed us to capture volumetric data at high throughput while maintaining synaptic resolution. Another advantage of using a Bessel focus for *in vivo* brain imaging is the robustness of this volumetric imaging tool against axial motion. With an axially extended focus as the excitation, structures of interest can remain within the imaged volume even in the presence of small axial displacements of the sample, which are otherwise not straightforward to correct for with a Gaussian focus [18].

Acknowledgments

We thank the Ji lab for helpful discussions, and Erminia Fardone for cutting the brain slices.

Funding. Howard Hughes Medical Institute; National Institutes of Health (NIH) (U01 NS103573, U01 NS103489, U01NS103571).

References

1. Denk W, Strickler JH, Webb WW. Two-photon laser scanning fluorescence microscopy. Science. 1990; 248:73–76. [PubMed: 2321027]
2. Horton NG, Wang K, Kobat D, Clark CG, Wise FW, Schaffer CB, Xu C. In vivo three-photon microscopy of subcortical structures within an intact mouse brain. Nat Photon. 2013; 7:205–209.
3. Ouzounov DG, Wang T, Wang M, Feng DD, Horton NG, Cruz-Hernandez JC, Cheng YT, Reimer J, Tolias AS, Nishimura N, Xu C. In vivo three-photon imaging of activity of GCaMP6-labeled neurons deep in intact mouse brain. Nat Meth. 2017; 14:388–390.

4. Tao X, Lin HH, Lam T, Rodriguez R, Wang JW, Kubby J. Transcutical imaging with cellular and subcellular resolution. Biomed Opt Express. 2017; 8:1277–1289. [PubMed: 28663828]
5. Grienberger C, Konnerth A. Imaging Calcium in Neurons. Neuron. 2012; 73:862–885. [PubMed: 22405199]
6. Ji N, Freeman J, Smith SL. Technologies for imaging neural activity in large volumes. Nature Neurosci. 2016; 19:1154. [PubMed: 27571194]
7. Welford WT. Use of Annular Apertures to Increase Focal Depth. J Opt Soc Am. 1960; 50:749–753.
8. Thériault G, Koninck YD, McCarthy N. Extended depth of field microscopy for rapid volumetric two-photon imaging. Opt Express. 2013; 21:10095–10104. [PubMed: 23609714]
9. Thériault G, Cottet M, Castonguay A, McCarthy N, De Koninck Y. Extended two-photon microscopy in live samples with Bessel beams: steadier focus, faster volume scans, and simpler stereoscopic imaging. Front Cell Neurosci. 2014; 8:139. [PubMed: 24904284]
10. Lu R, Tanimoto M, Koyama M, Ji N. 50 Hz volumetric functional imaging with continuously adjustable depth of focus. BioRxiv, 240069. 2017
11. Botcherby EJ, Juškaitis R, Wilson T. Scanning two photon fluorescence microscopy with extended depth of field. Opt Commun. 2006; 268:253–260.
12. Lu R, Sun W, Liang Y, Kerlin A, Bierfeld J, Seelig JD, Wilson DE, Scholl B, Mohar B, Tanimoto M, Koyama M, Fitzpatrick D, Orger MB, Ji N. Video-rate volumetric functional imaging of the brain at synaptic resolution. Nature Neurosci. 2017; 20:620. [PubMed: 28250408]
13. Akturk S, Gu X, Kimmel M, Trebino R. Extremely simple single-prism ultrashort-pulse compressor. Opt Express. 2006; 14:10101–10108. [PubMed: 19529405]
14. Horton NG, Xu C. Dispersion compensation in three-photon fluorescence microscopy at 1,700 nm. Biomed Opt Express. 2015; 6:1392–1397. [PubMed: 25909022]
15. Turcotte R, Liang Y, Ji N. Adaptive optical versus spherical aberration corrections for in vivo brain imaging. Biomed Opt Express. 2017; 8:3891–3902. [PubMed: 28856058]
16. Ji N. Adaptive optical fluorescence microscopy. Nat Meth. 2017; 14:374–380.
17. Sinefeld D, Paudel HP, Ouzounov DG, Bifano TG, Xu C. Adaptive optics in multiphoton microscopy: comparison of two, three and four photon fluorescence. Opt Express. 2015; 23:31472–31483. [PubMed: 26698772]
18. Andermann M, Kerlin A, Reid C. Chronic cellular imaging of mouse visual cortex during operant behavior and passive viewing. Front Cell Neurosci. 2010; 4:3. [PubMed: 20407583]

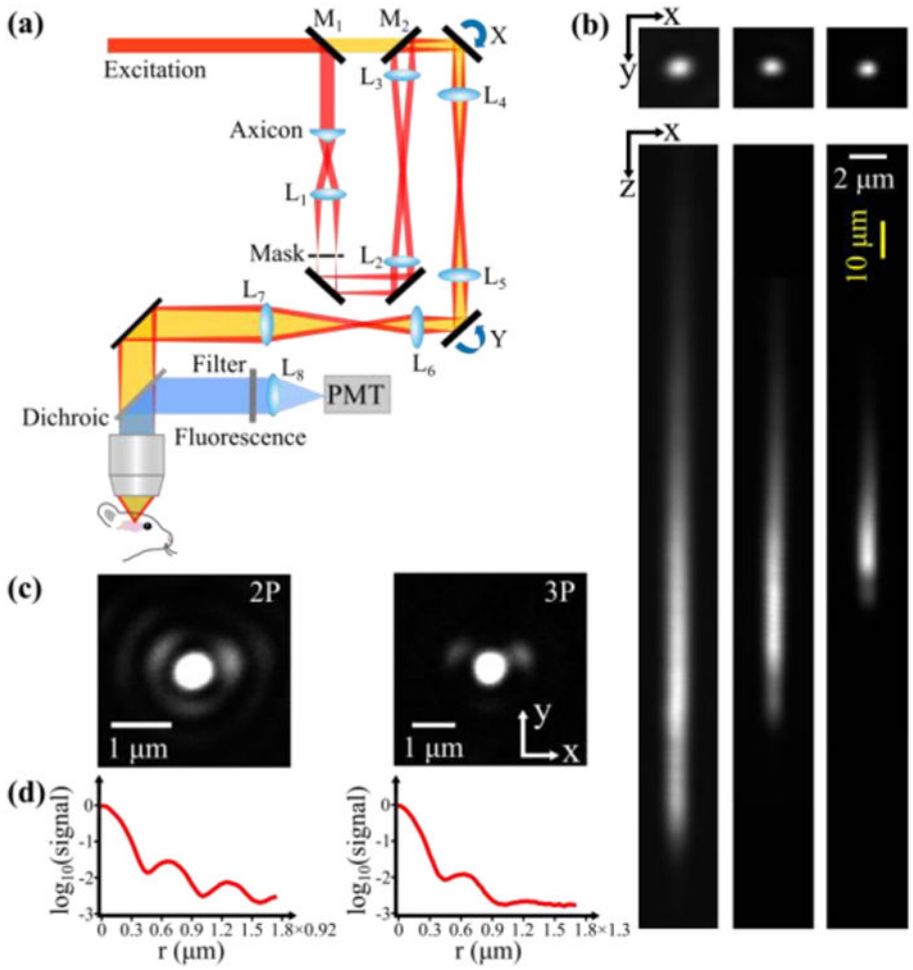

Fig. 1.

Three-photon fluorescence microscopy with a Bessel focus. (a) Schematics of our homebuilt three-photon microscope with an axicon-based Bessel module. Flip mirrors M_1 and M_2 allow switching between Gaussian (yellow path) and Bessel (red path) imaging modalities. L, lenses; X and Y, galvanometers; PMT, photomultiplier tube.(b) Three-photon images of a 1-μm-diameter red fluorescent bead excited with different Bessel foci under 1300 nm excitation: (left) NA = 0.48, focal length L_1 = 100 mm, L_2 offset = -10 mm; (center) NA = 0.6, focal length L_1 = 125 mm, L_2 offset = -10 mm; (right) NA = 0.72, focal length L_1 = 150 mm, L_2 offset = 0 mm. Post-objective powers: 15.5, 4.9, and 3.2 mW, respectively. Note the different scales for the lateral and axial scale bars. (c) Images of a 0.2-μm-diameter red fluorescent bead taken under (left) two- and (right) three-photon excitation with a Bessel focus of 0.96 NA and axial FWHM of 10 μm (focal length of L_1 = 200 mm, L_2 offset = -10 mm), under 920 and 1300 nm excitation, respectively. Contrast was enhanced 7× to highlight the side rings in both images. Post-objective powers: 10 and 16.7 mW, respectively.(d) Signal profiles (obtained from a radial average and plotted in logarithmic scale) of images in (c). With three-photon excitation the side rings (typical of high-NA Bessel foci) are more effectively suppressed.

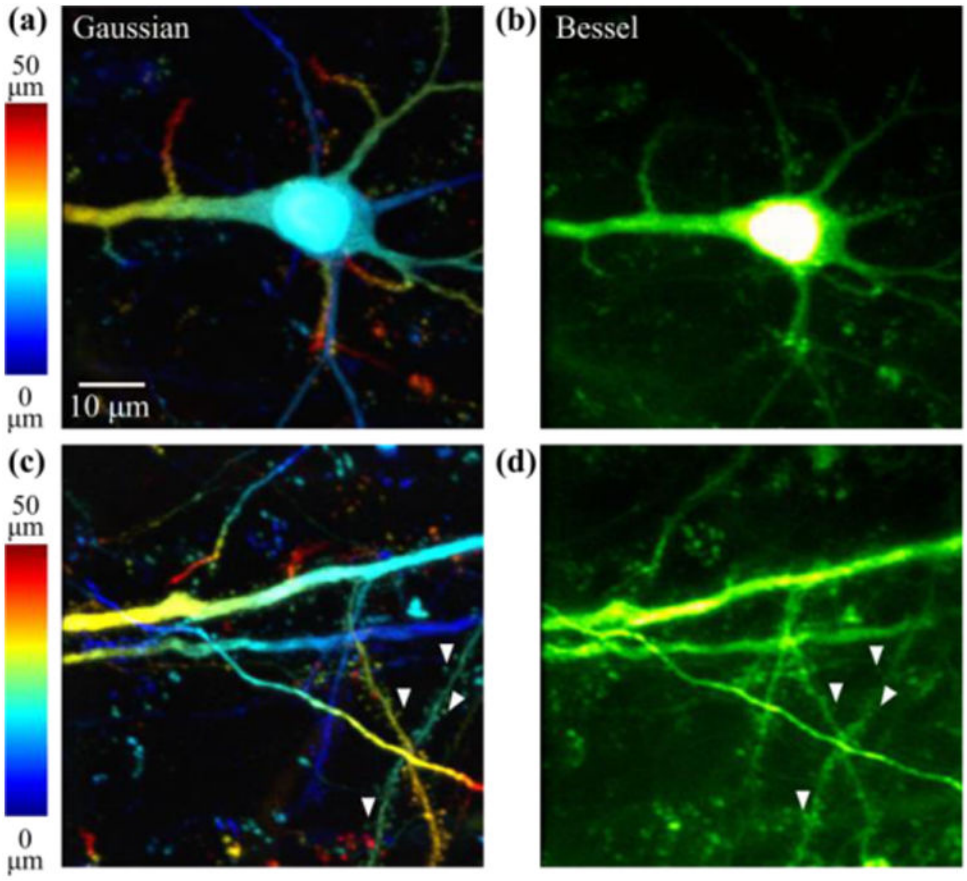

Fig. 2.

Three-photon fluorescence microscopy with Bessel focus scanning captures fine structures in volumes of mouse (Thy1-GFP line M) brain slices. (a,c) Maximum intensity projections of a 50-µm thick image stack obtained with a Gaussian focus, with a 2-µm axial step size, color-coded by depth, under 1300 nm excitation.Post-objective power: 2.8 mW. (b,d) Images of the same volumes as (a,c), respectively, obtained with a Bessel focus of NA 0.6 and axial FWHM of 36 µm. Post-objective powers: 25 and 38 mW, respectively.

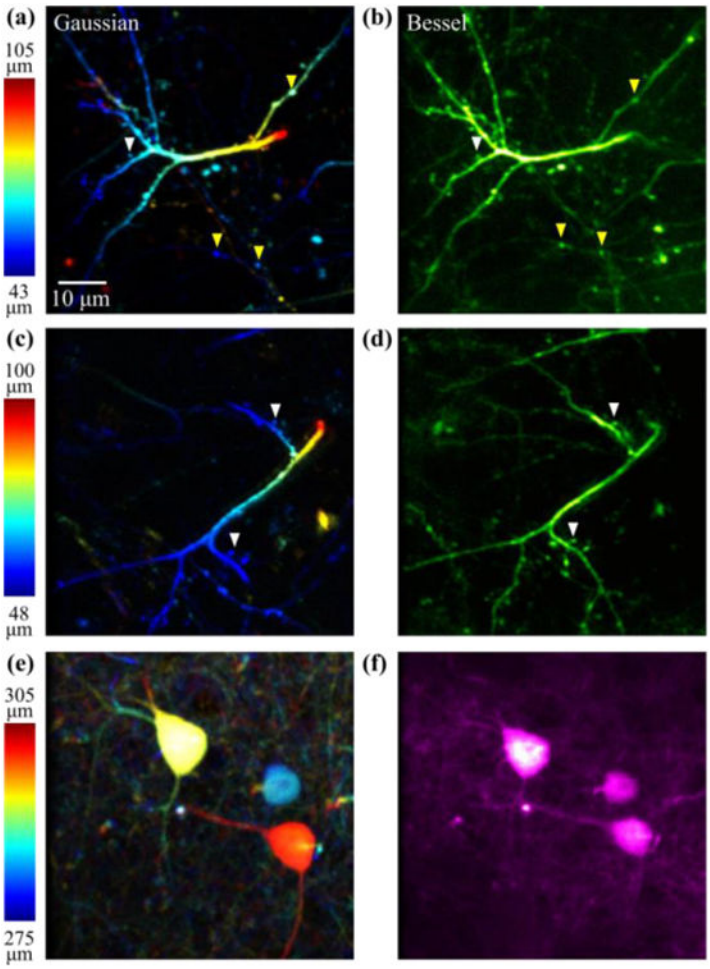

Fig. 3.

In vivo volumetric three-photon fluorescence microscopy of micebrains. Maximum intensity projection of a (a) 62-µm and (c) 52-µm thick volume at ~80 µm below dura, color-coded by depth, imaged with a Gaussian focus, at a2-µm axial step size, under 1300 nm excitation. Post-objective powers: 3 and 4 mW, respectively. (b,d) Image of the same volume as (a,c), respectively, obtained with a Bessel focus of NA 0.6 and axial FWHM of 38 µm.White arrowheads label dendritic spines, and yellow arrowheads label axonal boutons.Post-objective powers: 30 and 40 mW, respectively.(e) Maximum intensity projection of a 30-µm thick volume at ~290 µm below dura, color-coded by depth, imaged with a Gaussian focus, at a2-µm axial step size, under 1700 nm excitation. Post-objective power: 15 mW. (f) Image of the same volume as (e) obtained with a Bessel focus of NA 0.6 and axial FWHM of 27 µm. Post-objective power: 73 mW.A Thy1-GFP line M mouse was used for (a-d), and a Gad2-IRES-Cre × Ai14 for(e,f).